PCCP

Accepted Manuscript

ROYAL SOCIETY OF CHEMISTRY

www.rsc.org/pccp

PCCP Guidelines for Referees

Physical Chemistry Chemical Physics **(*PCCP*) is a high quality journal with a large international readership from many communities**

Only very important, insightful and high-quality work should be recommended for publication in *PCCP*.

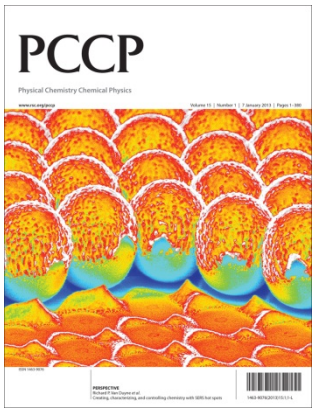

To be accepted in *PCCP* - a manuscript must report:

- Very high quality, reproducible new work
- **Important new physical insights** of significant general interest
- A novel, stand-alone contribution

Routine or incremental work should not be recommended for publication. Purely synthetic work is not suitable for PCCP

If you rate the article as 'routine' yet recommend acceptance, please give specific reasons in your report.

Less than 50% of articles sent for peer review are recommended for publication in *PCCP*. The current PCCP Impact Factor is 3.83

PCCP is proud to be a leading journal. We thank you very much for your help in evaluating this manuscript. Your advice as a referee is greatly appreciated.

With our best wishes,

Philip Earis (pccp@rsc.org)
Managing Editor, PCCP

Prof Daniella Goldfarb
Chair, PCCP Editorial Board

General Guidance (For further details, see the RSC's Refereeing Procedure and Policy)

Referees have the responsibility to treat the manuscript as confidential. Please be aware of our **Ethical Guidelines** which contain full information on the responsibilities of referees and authors.

When preparing your report, please:
• Comment on the originality, importance, impact and scientific reliability of the work;
• State clearly whether you would like to see the paper accepted or rejected and give detailed comments (with references) that will both help the Editor to make a decision on the paper and the authors to improve it;

Please inform the Editor if:
• There is a conflict of interest;
• There is a significant part of the work which you cannot referee with confidence;
• If the work, or a significant part of the work, has previously been published, including online publication, or if the work represents part of an unduly fragmented investigation.

When submitting your report, please:
• Provide your report rapidly and within the specified deadline, or inform the Editor immediately if you cannot do so. We welcome suggestions of alternative referees.

Richard Rosenberg
Staff Scientist
Magnetic Materials Group
X-ray Science Division
Advanced Photon Source
Argonne National Laboratory
9700 South Cass Avenue, Bldg. 401
Argonne, IL 60439

1-630-252-6112 phone
1-630-252-7392 fax
rar@aps.anl.gov

May 8, 2014

We would like to thank the referees for their positive comments and suggestions. In the revised manuscript we have made the following changes (highlighted in yellow on the marked up version).

Referee 1:
(i) In the Introduction it is stated that the unthiolated DNA acts with the substrate through the bases. On the other hand, both DNAs protrude by about 45 degrees from the surface, so this substrate-base interaction only concerns a few bases near the Au-N coupling?

We have changed the sentence on page 8 from:
"For uDNA bonding to the Au substrate likely occurs through a primary amine group on one of the bases, most likely the adenine bases."
To:
For uDNA bonding to the Au substrate likely occurs through a primary amine group on one of the bases, most likely the adenine bases located at the end of the strand.

(i) In the second sentence of the Introduction I suggest to replace “resonant scattering” by “resonant attachment”

This was done.

Referee 2:
Change the second sentence of the introduction: “These electrons are produced via a cascade process following the ionization of a core (deeply bound) electron”. This statement may be ambiguous for those not familiar with this process. I suggest writing “In the case of primary electromagnetic radiation, these electrons are produced by small and successive energy losses of the initial photoelectrons »,

This sentence was changed to:
"In the case of primary electromagnetic radiation, the SEs are produced by small and successive energy losses (inelastic scattering) of the initial photo or Auger electrons. "

Also erase the word “by” in the 7th line of the introduction as it is repeated.

This was done.

We hope the manuscript is now suitable for publication. Thank you.

Sincerely,
Richard Rosenberg

Submitted to PCCP

The relationship between interfacial bonding and radiation damage in adsorbed DNA

R. A. Rosenberg[1], J. M. Symonds[2], K. Vijayalakshmi [1], Debabrata Mishra[3], T. M. Orlando[2] and R. Naaman[3]

[1]Advanced Photon Source, Argonne National Laboratory, 9700 S. Cass Ave., Argonne, IL 60439

[2]School of Chemistry and Biochemistry and School of Physics, Georgia Institute of Technology, Atlanta, Georgia 30332

[3] Department of Chemical Physics, Weizmann Institute, Rehovot 76100, Israel

We have performed a comparison of the radiation damage occurring in DNA adsorbed on gold in two different configurations, when the DNA is thiolated and bound covalently to the substrate and when it is unthiolated and interacts with the substrate through the bases. Both molecules were found to organize so as to protrude from the surface at ~45 degrees. Changes in the time-dependent C 1s and O 1s X-ray photoelectron (XP) spectra resulting from irradiation were interpreted to arise from cleavage of the phosphodiester bond and possibly COH desorption. By fitting the time-dependent XP spectra to a simple kinetic model, time constants were extracted, which were converted to cross sections and quantum yields for the damage reaction. The radiation induced damage is significantly higher for the thiolated DNA. N 1s X-ray absorption spectrum revealed the N-C=N LUMO is more populated in the unthiolated molecule, which is due to a higher degree of charge transfer from the substrate to this LUMO in

the unthiolated case. Since the N-C=N LUMO of the thiolated molecule is comparatively less populated, it is more effective in capturing low energy electrons resulting in a higher degree of damage.

INTRODUCTION

High energy ionizing irradiation produces large amounts of low energy (<20 eV) secondary electrons (SEs). In the case of primary electromagnetic radiation, the SEs are produced by small and successive energy losses (inelastic scattering) of the initial photo or Auger electrons. Due to their low energy there is a high probability for the SEs to become trapped in antibonding orbitals, via resonant attachment, forming a temporary negative ion (TNI) resonance. If the lifetime of the TNI state is long enough, then bond rupture can occur by a process known as dissociative electron attachment (DEA). Sanche and coworkers showed how low-energy electrons produce complex DNA damage by a DEA process.[1] Electrons that have slowed down to energies too low to induce ionization of DNA undergo resonant attachment to DNA bases. It has been shown that these electrons, once captured, are efficiently transferred to the sugar-phosphate backbone,[2, 3] causing the breaking of one or both strands of the DNA. One electron can in this way produce multiple lesions, thus amplifying the clustering of damage induced in DNA by a single radiation track.[4] Clustered lesions are difficult for the cell to repair and are therefore more likely to lead to permanent damage to the genome.[5] Recent work using Raman microspectroscopy has shown that substrate interactions and the specific base

pair sequence affects the single strand break probability via low energy (< 5 eV) shape resonances.[6]

Radiation therapy and radiosensitization applications take advantage of the fact that the local environment and bonding of DNA can have a profound impact on the effectiveness of low energy electrons. For instance it has been shown that binding of just two cisplatin molecules to a 3,197 base pair plasmid increases the number of single strand breaks caused by 10 eV electrons by nearly four times.[7] Also, the insertion of gold nanoparticles in the vicinity of DNA in cancer cells can lead to an increase in the number of low energy secondary electrons. The gold nanoparticles preferentially concentrate in subcutaneous tumors and thus have applications as radiosensitizers in cancer treatment.[8] Furthermore, the orientation of DNA on the gold surface has been shown to affect the OH^- yield induced by low energy electrons.[9] However, the effect of the DNA-gold bond on the reaction rate has not been studied.

There is vast literature on the role of TNI states and DEA in DNA related radiation chemistry.[10-14] We have recently found that if the SEs are spin polarized, then chiral-specific radiation chemistry may result.[15] Due to its high flux density, synchrotron radiation (SR) has often been used to induce and study radiation chemistry in numerous systems,[16] including DNA and related molecules.[17-24] SR has also been used to probe the electronic structure and bonding of such molecules, primarily by probing the occupied states with X-ray photoelectron spectroscopy (XPS) and the unoccupied

states with X-ray absorption (XAS) measurements. Bond overlap and localization can be revealed by XPS while XAS can determine the density of unoccupied states and the orientation of the orbitals.[25-37] Resonant photoemission (combining XPS and XAS) can be used to determine the lifetime of the excited state with 100 femtosecond precision.[38, 39] It is expected that the extent of occupation and the lifetime will play a critical role in determining the nature of the TNI state and thus the efficiency of the DEA process. However, to our knowledge there has been no direct study on the correlation between the lowest unoccupied molecular orbital (LUMO) occupation and radiation damage.

In the present paper we examine X-ray induced reactions of DNA adsorbed on a gold substrate when the DNA is either thiolated (tDNA) or when it is unthiolated (uDNA). By performing polarization-dependent X-ray absorption spectroscopy at the N K edge we determined that the thiolated DNA protrudes from the surface at ~45 degrees, in agreement with previous studies.[26, 40] We also found that the unthiolated molecules have a similar orientation. However, due to differences in charge transfer between the gold and the DNA in the two systems there is a higher density of unoccupied states in the N-C=N derived π* orbital for tDNA. We also found that the adsorbed tDNA has a significant higher cross section for radiation damage. The reason for this enhancement could arise from the greater probability of forming a TNI state for the tDNA due to the higher density of unoccupied π* states.

EXPERIMENTAL

The samples were prepared at the Weizmann Institute according to a method described previously.[41, 42] They consisted of 40 base pairs of 3' thiolated as well as unthiolated DNA on a clean 200 nm thick polycrystalline gold film on a Si substrate. The exact sequence was:

5' - TCT CAA GAA TCG GCA TTA GCT CAA CTG TCA ACT CCT CTT T -3'

3' - AGA GTT CTT AGC CGT AAT CGA GTT GAC AGT TGA GGA GAA A -5'

They were shipped in sealed vials under a nitrogen atmosphere to laboratories in the United States and not opened until shortly before they were loaded into a load lock chamber, which was immediately evacuated. Work functions of single-stranded variants were determined at the Weizmann Institute according to a method described previously.[43]

The measurements for these experiments were performed at two different synchrotron radiation sources. Experiments utilizing X-rays in the range 500 to 1000 eV were performed on beamline 4-ID-C at the Advanced Photon Source (APS). The angle (Φ) between the incoming X-ray beam and the sample surface was 55 degrees and the emitted electrons were detected by a CLAM 2 electron energy analyzer, oriented at an angle θ of 35 degrees (Fig. 1) and operated at a pass energy of 50 eV, except for the P 2p results, which were obtained using 100 eV pass energy. All X-ray photoelectron spectroscopy (XPS) data were taken at

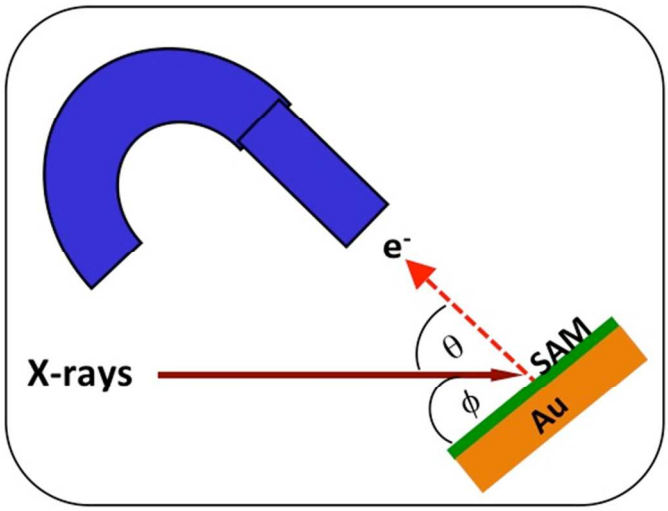

Figure 1. Schematic diagram of the experimental setup.

a photon energy of 950 eV. The total electron yield (TEY) from the electrically isolated sample was determined by measuring the restoring current using a current amplifier. The APS measurements were performed with the storage ring operating in “top up” mode so the X-ray flux density was constant to within 1-2 % during all measurements at a given energy. XPS and polarization-dependent near-edge X-ray absorption fine structure (NEXAFS) measurements at the N K edge (400 eV) were carried out on the HERMON beamline at the Synchrotron Radiation Center (SRC). NEXAFS data were acquired by measuring the TEY emitted from the sample. The spectra were normalized to the beamline flux by measuring the electron yield from a partially transmitting gold mesh inserted into the X-ray beam. To minimize possible effects of radiation damage, each NEXAFS scan was acquired at a fresh spot on the sample. XPS data were

acquired with a cylindrical mirror electron energy analyzer (CMA) oriented at 90 degrees with respect to the incident photon beam.

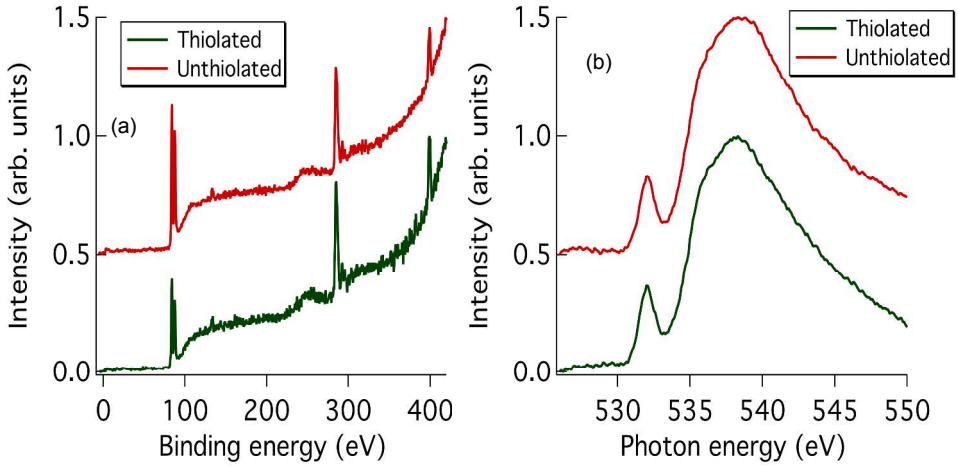

Figure 2. (a) Survey XPS spectra of thiolated (bottom) and unthiolated (top) DNA adsorbed on Au taken with 500 eV photons at the SRC. (b) O 1s X-ray absorption spectra of thiolated (bottom) and unthiolated (top) DNA adsorbed on Au taken at the APS.

Characterization of the samples was done at both APS and SRC. Figure 2(a) shows survey XPS spectra of tDNA and uDNA acquired using 500 eV X-rays at SRC. Both samples show characteristic C 1s (285 eV) and N 1s (400 eV) DNA peaks as well as Au 4f peaks (~84 eV) from the substrate. Note that the DNA signals are stronger and the Au 4f peaks are smaller for tDNA indicating that the tDNA coverage is slightly higher than that of uDNA. Oxygen K X-ray absorption spectra of both samples, obtained at the APS, are shown in Fig. 2(b).

Both spectra are similar to each other and to previously reported results.[17, 19, 34, 37, 44, 45]

RESULTS AND DISCUSSION

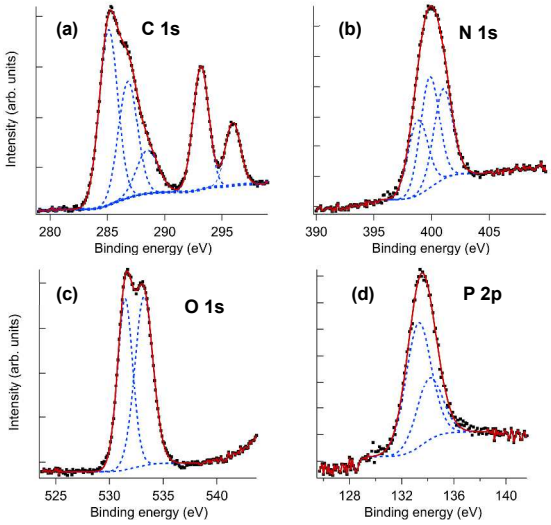

Figure 3. Core level XPS of thiolated DNA adsorbed on Au taken with 950 eV X-rays at the APS. (a) C 1s and K 2p (b) N 1s (c) O 1s (d) P 2p. The points are the experimental data, the dashed lines are fits to individual components (see Table 1) and the solid line is the fitted envelope.

Core level XPS data obtained at 950 eV at APS from tDNA are shown in Fig. 3. These spectra are the result of signal averaging up to 30 individual spectra taken at the same position. During the course of these measurements significant changes were observed in the individual components that make up the spectral envelope in the case of C 1s (a) and O 1s (c), but not for N 1s (b) and P 2p (d). These changes will be dealt with in depth later in the paper. The results shown in Fig. 3 are similar to previously reported spectra of DNA and related

molecules.[25, 29, 32, 46, 47] Due to the complex chemical environment of the C, N, O atoms in DNA each core level peak is composed of two or more components. To gain insight into the energies of these components, curve-fitting techniques were employed. For these spectra most of the peak width is due to instrumental broadening, so the peaks were fit using components that carried a 10 % Lorentzian, 90 % Gaussian peak shape. The minimum number of components that resulted in a reasonable fit was utilized. These components, along with their assignments, are shown in Table 1. The spectra and their components are in reasonable agreement with previously reported results,[29, 48] considering the lower resolution of the present work.

Polarization-dependent N NEXAFS obtained using linearly polarized light from both forms of DNA are shown in Fig. 4. The two sharp peaks at 399 and 401 eV are due to N 1s excitation to π* orbitals which are localized on the base pairs, while the broad peak at 407 eV is due to excitation to σ* orbitals. The 401 eV peak has been assigned to core level excitation of a nitrogen bound to a carbonyl group and the 399 eV peak arises from excitation of the remaining nitrogen atoms.[29] As the angle between the X-ray beam and the sample normal increases, the E vector becomes more aligned with the π* orbitals of the base pairs for the protruding DNA. This enhances the N 1s ➔ π* intensity as has been observed in previous studies on tDNA.[26, 30, 33] To our knowledge there have been no previously reported polarization-dependent N NEXAFS studies on uDNA, such as those shown in Fig. 4(b). The spectra of the two types of DNA are similar except for the enhancement of the 399 eV peak in the case of tDNA. To

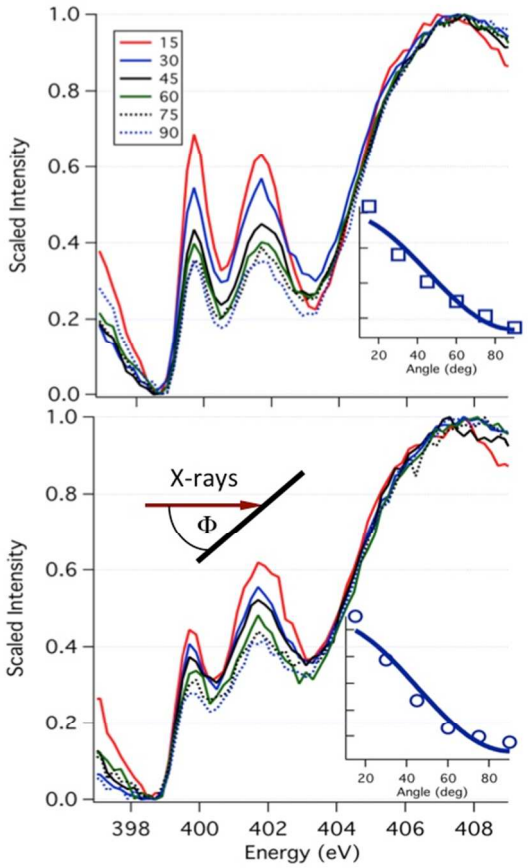

Figure 4. Polarization-dependent N 1s X-ray absorption spectra of thiolated (top) and unthiolated (bottom) DNA adsorbed on Au taken at the SRC. The insets show the angular dependence of the π* resonance at 399 eV for thiolated DNA and 401 eV for unthiolated DNA. The symbols are the experimental data and the straight line is a fit to the model discussed in the text.

determine the orientation of the DNA on the gold surface, the areas of the 399 eV peak (tDNA) and the 401 eV peak (uDNA) were extracted using curve fitting techniques.[49] These areas are plotted as a function of angle in the insets of Figs.

4(a) and 4(b). For 100% linearly polarized light, the following equation describes the angular (θ) dependence of the π* orbital:[27]

$$I(\theta) = A/3*[1+1/2*(3\cos^2(\theta)-1)(3\cos^2(\alpha)-1)]$$

A is a constant, θ is the angle between the polarization vector and the sample normal, and α is the polar angle between the vector of the π* orbital and the surface normal. The solid line in the insets in Fig. 4 is a fit to this equation and yields angles α of 43° ± 2° for tDNA and 44° ± 2° for uDNA, which is in agreement with previously reported results for tDNA.[26, 40] Therefore, the two types of DNA are oriented in a similar fashion, although the coverage is lower for uDNA.

NEXAFS spectra map out the local density of unoccupied states. The differences in the spectra between the two types of DNA seen in Fig. 4 reveal changes in the N-related unoccupied levels that occur as a result of dissimilar substrate-bonding interactions. For tDNA it is well established that bonding to the gold substrate occurs through the thiol group,[50] which results in a net transfer of holes to the tDNA and electrons to the gold.[42] Polarization modulation infrared reflection absorption spectroscopy data obtained on these samples also indicate strong gold-base interaction (see Supplementary Information). For uDNA bonding to the Au substrate likely occurs through a primary amine group on one of the bases,[51-53] most likely the adenine bases located at the end of the strand.[46] The Au-N bond has a weaker binding strength and higher contact resistance than the Au-S bond,[54] which should result in less charge transfer between the Au and

the uDNA. This is reflected in the NEXAFS spectra in Fig. 4; the greater intensity of the 399 eV peak for tDNA as compared to uDNA is due to more holes being injected into the tDNA through the Au-S bond. Analogous changes in N 1s → π* intensity have been seen for N_2O adsorbed on a metal surface where the peak intensity resulting from excitation to an orbital localized on a particular N atom was reduced when that atom was coupled to the surface.[55] The increased electron transfer from tDNA to gold is also supported by our work function measurements made on single-stranded variants. For the bare gold surface the work function was found to be 4.88 eV, for the thiolated sample it was 4.45eV, while for the unthiolated DNA it was 4.57 eV (all measurement errors are less than 0.05 eV).

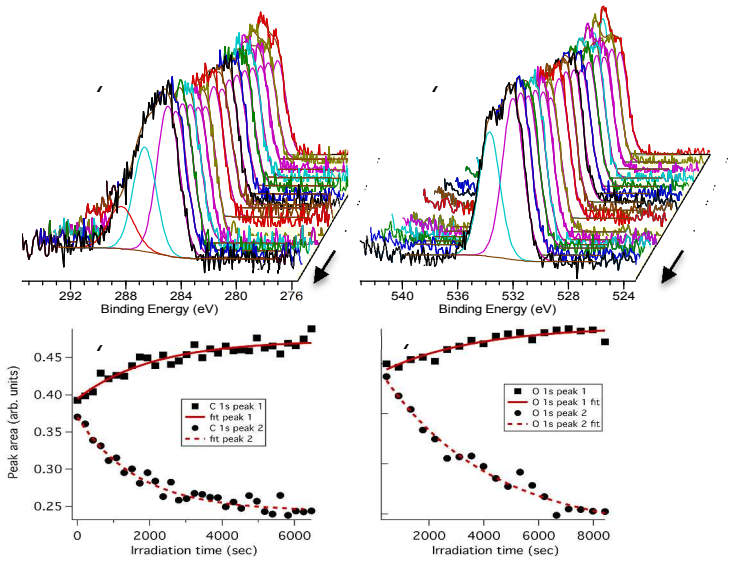

Figure 5. Series of irradiation time-dependent XP spectra: (a) C 1s (b) O 1s. Also shown are the deconvoluted spectral components. Irradiation time dependence of the areas of peaks 1 and 2 (see Table 1) for (c) C 1s (d) O 1s. The symbols

are the experimental data and the straight line is a fit to the model discussed in the text.

Irradiation time-dependent C 1s and O 1s XPS spectra for tDNA are shown in Fig. 5(a) and (b). The peak-fit extracted areas of components 1 and 2 (Table 1) are plotted as a function of irradiation time in Fig. 5(c) and (d). Component 1 for C (C-C, C=C) and O (C=O, P=O, P-O^-(K^+)) increased and component 2 (C: C-O, C-N, C-NH_2, N-C-N, N=C-N) (O: C-O-P, C-O-C) decreased with time, but the attenuation of component 2 was higher than the rise in component 1. Component 3 of the C 1s data also decreased with time, but due to its weak intensity the data were noisier than that of component 2. The overall intensities of the C 1s and O 1s peaks decreased by ~10 %. No significant changes were observed in the N 1s or P 2p XPS spectra under these conditions. Using the kinetic relationship, $I = I_0\exp(-t/\tau)$, where I = peak area; I_0 = initial peak area; t = time, we are able to extract the time constants, τ, for the reactions resulting in a decrease in the area of a component. Similar first order kinetic treatment yields the equation $I = I_0(1-\exp(-t/\tau))$ for components that increase.[56] Results of fitting the data to these equations are shown as the lines in Fig. 5(c) and 5(d). The derived time constants for the decreasing and increasing components for both C 1s and O 1s XPS data were the same, within experimental error.

Based on the assignments in Table 1, the decay of peak 2 in the C 1s spectra indicates the loss of C-O or C-N bonds and the rise in peak 1 indicates the formation of C-C or C=C species. Similarly the changes in the O 1s spectra indicate the loss of C-O-P and C-O-C species and the formation of C=O, P=O, or $P\text{-}O^{-}(K^{+})$ bonds. The similarity of the time constants for all the reactions suggests that these processes are correlated. Since no significant changes were observed in the N 1s spectra, reactions involving the base pairs appear to play a minor role under these conditions. Fission of the $C\text{-}NH_2$ bond would lead to an overall decrease in intensity, and loss of carbonyl species would result in changes of the relative intensities of peak 1 and peak 2. Cleavage of the *N*-glycosidic bond is also consistent with this data. However, due to the relatively poor resolution, slight changes in the relative intensities of the two components of the N 1s spectra would not be noticeable, but it is clear that there was no significant loss of N-containing species during the reaction.

In previous time-dependent XPS measurements of X-ray irradiated DNA,[47] Ptasinska, *et al* observed behavior that differed from that of the present work. They reported a significant decrease in the O 1s signal and smaller reductions in the N 1s and P 2p intensities; the overall C 1s signal increased. These experiments were performed using a laboratory XPS system and fairly thick films of plasmid or calf thymus DNA on Si or Ta substrates. Xiao, *et al* also reported time-dependent XPS results[57] at variance with the present study in the cisplatin-DNA system. They showed an ~50% decrease in the O and C 1s signals and ~20% reduction in N 1s and P 2p intensities following 3 hours of irradiation with a

laboratory x-ray source. Since it has been shown that substrate-DNA interactions[6, 9] and morphology[58] can have a profound effect on its radiation chemistry, it is not surprising that the present results are not consistent with this previous work.

The amount of water coadsorbed with the DNA can also influence the radiation chemistry.[10, 59] Although these measurements were made under ultra-high vacuum conditions, it is possible that some water remained. However, there is no indication of a water peak at ~535.4 eV[60] in the O 1s XPS data in Fig. 3(c), so it should not be a major factor.

It has been well established that one of the main mechanisms for low energy electrons to produce strand breaks (SBs) in DNA is by phosphodiester bond cleavage.[11, 12, 61, 62] The mechanism is thought to involve decay of the transient radical anion of the phosphate π* orbital to the strongly dissociative C-O σ* orbital.[62] This would result in loss of C-O-P species, formation of $P\text{-}O^-$ and C-C• bonds and would be consistent with the results shown in Fig. 5. If the reaction also led to COH loss by decomposition of the sugar molecule,[47, 63] this could account for the 10 % decrease in overall C 1s and O 1s XPS signals. Although it is not possible to rule out other minor pathways, such a reaction scheme should be a major factor in the overall X-ray induced reaction.

By performing numerous measurements of the time constants for the decay rate of component 2 of the C 1s peak (Fig. 5(c)), it was possible to extract cross sections for the reaction for both tDNA and uDNA. The cross sections (σ)

were determined using the relationship $\sigma = 1/\tau * f$, where τ is the time constant and f is the flux density. A photodiode was used to measure the flux and the beam size was determined using a wire scanner; the resulting flux density was 2 $x10^{14}/cm^2$. Since secondary electrons are thought to play a prominent role in the reaction, cross sections for electron-induced reactions were also determined by measuring the TEY for the samples and converting it into an electron flux density using the measured spot size. Due to the lower coverage, the TEY for uDNA was ~30% higher than for tDNA. To take into account the differences in coverage from spot to spot and from sample to sample, the quantum yield (QY) was also calculated by multiplying σ by the surface coverage.[64] The coverage was taken to be proportional to the total C 1s peak area for the first spectrum of a given photolysis series, and the average coverage for tDNA was set to 1.4 x 10^{13} molecules/cm^2.[2] Results of these calculations for tDNA and uDNA using both the photon and electron flux density are shown in Table 2. Although the given absolute cross sections and quantum yields may have large systematic errors, due to uncertainties in measurements of the coverage, x-ray beam size and flux, the relative values should be accurate to within the stated uncertainties. Despite the systematic errors, note that the absolute cross sections are in the same range as those reported for DEA to 2-deoxyribose,[65] and the per-nucleotide value for plasmid DNA.[66]

The overall conclusion from the results in Table 2 is that the radiation damage process is more efficient for tDNA as compared to uDNA. The ratios of the σ or QY values for thiolated versus unthiolated range from 1.2 ± 0.1 to 1.9 ±

0.2. A possible reason for this effect may be gleaned by examination of the N 1s X-ray absorption data shown in Fig. 4. Due to the relatively strong coupling between tDNA, as compared to uDNA, and the gold susbtrate, more holes are injected into tDNA. For Au-S the bond strength is ~40 kcal/mol, while for Au-N the bond strength is estimated to be 8 kcal/mol.[54] As a result there is a significantly higher density of unoccupied states for the lowest unoccupied molecular orbital (LUMO) associated with the N-C=N states for tDNA, as revealed by the greater intensity of the peak at 399 eV.[29] Similar phenomenon in which the gold substrate contributes to the adsorbate's state was observed for semiconductor nanoparticles adsorbed on gold via alkyldithiols.[67]

Therefore, due to the higher N-C=N LUMO density for tDNA, there is a greater probability for capture of a low energy secondary electron generated by the X-rays. It has been shown that low energy electron induced SBs in DNA depend on the electron capture probability of the DNA bases. Once captured, the electrons transfer from the base to the phosphate group and cause C-O bond rupture by a DEA process.[62, 68-70] Experiments and theory indicate that the process is enhanced by excitation of π* shape resonances and/or Feshbach resonances.[6, 11, 12, 59, 62, 71] Electron transmission measurements indicate that the number of guanine bases controls the electron capturing efficiency, perhaps as the result of its large dipole moment.[2, 3, 43] The present study is the first to correlate the radiation damage process with the nature of the unoccupied states in two DNA species that differ only in the way they are bound to the surface. Our

results support the importance of low-lying π* states in radiation damage caused by low energy electrons.

CONCLUSIONS

In summary, we have examined the X-ray induced radiation chemistry of the same double stranded DNA molecule adsorbed on a gold surface in two different configurations. The first is indirectly bonded via a thiol group whereas the second involves direct, though weaker adsorption, via the nitrogen on a base such as adenine. By examining polarization-dependent N 1s X-ray absorption spectra, both species were found to be oriented to the surface at ~45 degrees, but the thiolated DNA had a higher density of LUMO states. Time-dependent XPS spectra revealed changes in the C-O bonding following irradiation, which were thought to be the result of the interaction of low energy secondary electrons. The results are consistent with a model involving cleavage of the phosphodiester bond and possibly COH loss by decomposition of the sugar molecule. Time constants for the reaction were obtained by fitting the time-dependent XPS data to a simple kinetic model, which were then converted to cross sections and quantum yields for the reaction. The overall reaction rate is significantly higher for the thiolated DNA, which we conjecture is a result of its higher density of LUMO states. This leads to more efficient capture of the low energy electrons by the bases, hence to a higher degree of phosphodiester bond cleavage following electron transfer to the phosphate group. It is interesting to note that one of the main differences between the present results and prior studies of X-ray damage on thick DNA films is that little or no reactions involving N were observed here,

whereas substantial N radiation chemistry was observed in the thick film work. We speculate that directly bonding the DNA to the substrate in the present work may shorten the lifetime of the repulsive state that leads to nitrogen release, thereby effectively quenching that reaction. These studies emphasize the importance of understanding the influence of local bonding in biomolecules in order to comprehend the manner in which low energy electrons produced by irradiation induce chemical reactions in these systems.

Acknowledgements

The work performed at the Advanced Photon Source was supported by the U.S. Department of Energy, Office of Science, Office of Basic Energy Sciences under Contract No. DE-AC02-06CH11357. This work is based in part upon research conducted at the Synchrotron Radiation Center, University of Wisconsin-Madison, which is supported by the National Science Foundation under Award No. DMR-0537588. TMO and JMS wish to acknowledge support from the U.S. Department of Energy, Office of Basic Energy Sciences under Contract No. DE-FG02-02ER15337. We would like to thank Nir Eliyahu and Tal Markus for experimental support.

Table 1: Binding energies of the components in Figure 3 and their chemical assignments.[29]

Core level	Peak	|BE (eV)	Chemical moiety
C 1s	1	285.1	C-C, C=C
	2	286.8	C-O, C-N, C-NH_2, N-C-N, N=C-N
	3	288.5	N-C-O, N-C=O, N-C(=O)-N
N 1s	1	399.6	C-NH_2, C=N-C
	2	401.1	N-C-O, N-C=O
O 1s	1	531.5	C=O, P=O, P-$O^-(K^+)$
	2	533.2	C-O-P, C-O-C
P 2p	1	133.3	$2p_{3/2}$
	2	134.1	$2p_{1/2}$

Table 2: Values of the cross section and quantum yield for tDNA and uDNA calculated using the X-ray or electron flux density.

	Thiolated (t)	Unthiolated (u)	Ratio (t/u)
X-ray cross section (Mb)	3.1± 0.2	2.5 ± 0.2	1.2 ± 0.1
Electron cross section (Mb)	5.5 ± 0.3	3.6 ± 0.3	1.5 ± 0.1
X-ray quantum yield (x10^{-5})	4.0 ± 0.2	2.6 ± 0.2	1.5 ± 0.1
Electron quantum yield (x10^{-5})	7.2 ± 0.4	3.7 ± 0.3	1.9 ± 0.2

REFERENCES

1. B. Boudaïffa, P. Cloutier, D. Hunting, M. A. Huels and L. Sanche, *Science*, 2000, **287**, 1658-1660.
2. S. G. Ray, S. S. Daube, H. Cohen and R. Naaman, *Isr. J. Chem.*, 2007, **47**, 149-159.
3. S. G. Ray, S. S. Daube and R. Naaman, *Proc. Nat. Acad. Sci. USA*, 2005, **102**, 15-19.
4. H. Nikjoo, P. O'Neill, D. T. Goodhead and M. Terrisol, *Int. J. Radiat. Biol.*, 1997, **71**, 467-483.
5. J. F. Ward, *Radiat. Res.*, 1985, **104**, S103-S111.
6. A. N. Sidorov and T. M. Orlando, *J. Phys. Chem. Lett.*, 2013, **4**, 2328-2333.
7. Y. Zheng, D. J. Hunting, P. Ayotte and L. Sanche, *Phys. Rev. Lett.*, 2008, **100**, 198101.
8. Y. Zheng, D. J. Hunting, P. Ayotte and L. Sanche, *Radiat. Res.*, 2008, **169**, 19-27.
9. X. Pan and L. Sanche, *Phys. Rev. Lett.*, 2005, **94**, 198104.
10. E. Alizadeh and L. Sanche, *Chem. Rev.*, 2012, **112**, 5578-5602.
11. I. Baccarelli, I. Bald, F. A. Gianturco, E. Illenberger and J. Kopyra, *Phys. Rep.*, 2011, **508**, 1-44.
12. J. Gu, J. Leszczynski and H. F. Schaefer, *Chem. Rev.*, 2012, **112**, 5603-5640.

13. R. Naaman and L. Sanche, *Chem. Rev.*, 2007, **107**, 1553-1579.

14. L. Sanche, *J. Phys. B: At. Mol. Opt. Phys.*, 1990, **23**, 1597.

15. R. A. Rosenberg, M. Abu Haija and P. J. Ryan, *Phys. Rev. Lett.*, 2008, **101**, 178301.

16. R. A. Rosenberg and S. P. Frigo, in Chemical Applications of Synchrotron Radiation, Part II: X-ray Applications, ed. T. K. Sham, World Scientific Publishing Co., Singapore, 2002, vol. 12A, ch. 9, p. 462.

17. K. Akamatsu and A. Yokoya, *Radiat. Res.*, 2001, **155**, 449-452.

18. K. Fujii, N. Shikazono and A. Yokoya, *J. Phys. Chem. B*, 2009, **113**, 16007-16015.

19. K. Fujii and A. Yokoya, *Radiat. Phys. Chem.*, 2009, **78**, 1188-1191.

20. P. S. Johnson, P. L. Cook, X. Liu, W. Yang, Y. Bai, N. L. Abbott and F. J. Himpsel, *J. Chem. Phys.*, 2011, **135**, 044702-044709.

21. A. Kade, K. Kummer, D. V. Vyalikh, S. DanzenbaÃàcher, A. BluÃàher, M. Mertig, A. Lanzara, A. Scholl, A. Doran and S. L. Molodtsov, *J. Phys. Chem. B*, 2010, **114**, 8284-8289.

22. G. Tzvetkov and F. P. Netzer, *J. Chem. Phys.*, 2011, **134**, 204704-204708.

23. J. Wang, C. Morin, L. Li, A. P. Hitchcock, A. Scholl and A. Doran, *J. Elec. Spec. Rel. Phen.*, 2009, **170**, 25-36.

24. Y. Zubavichus, O. Fuchs, L. Weinhardt, C. Heske, E. Umbach, J. D. Denlinger and M. Grunze, *Radiat. Res.*, 2004, **161**, 346-358.

25. N. Ballav, P. Koelsch and M. Zharnikov, *J. Phys. Chem. C*, 2009, **113**, 18312-18320.

26. J. N. Crain, A. Kirakosian, J. L. Lin, Y. Gu, R. R. Shah, N. L. Abbott and F. J. Himpsel, *J. Appl. Phys.*, 2001, **90**, 3291-3295.

27. K. Fujii, K. Akamatsu and A. Yokoya, *J. Phys. Chem. B*, 2004, **108**, 8031-8035.

28. W. Hua, B. Gao, S. Li, H. Ågren and Y. Luo, *J. Phys. Chem. B*, 2010, **114**, 13214-13222.

29. K. Kummer, D. V. Vyalikh, G. Gavrila, A. B. Preobrajenski, A. Kick, M. Bönsch, M. Mertig and S. L. Molodtsov, *J. Phys. Chem. B*, 2010, **114**, 9645-9652.

30. C.-Y. Lee, P. Gong, G. M. Harbers, D. W. Grainger, D. G. Castner and L. J. Gamble, *Anal. Chem.*, 2006, **78**, 3316-3325.

31. X. Liu, F. Zheng, A. Jürgensen, V. Perez-Dieste, D. Y. Petrovykh, N. L. Abbott and F. J. Himpsel, *Can. J. Chem.*, 2007, **85**, 793-800.

32. D. Y. Petrovykh, H. Kimura-Suda, M. J. Tarlov and L. J. Whitman, *Langmuir*, 2004, **20**, 429-440.

33. D. Y. Petrovykh, V. Pérez-Dieste, A. Opdahl, H. Kimura-Suda, J. M. Sullivan, M. J. Tarlov, F. J. Himpsel and L. J. Whitman, *J. Am. Chem. Soc.*, 2005, **128**, 2-3.

34. N. T. Samuel, C.-Y. Lee, L. J. Gamble, D. A. Fischer and D. G. Castner, *J. Elec. Spec. Rel. Phen.*, 2006, **152**, 134-142.

35. S. M. Schreiner, A. L. Hatch, D. F. Shudy, D. R. Howard, C. Howell, J. Zhao, P. Koelsch, M. Zharnikov, D. Y. Petrovykh and A. Opdahl, *Anal. Chem.*, 2011, **83**, 4288-4295.

36. D. V. Vyalikh, S. Danzenbächer, M. Mertig, A. Kirchner, W. Pompe, Y. S. Dedkov and S. L. Molodtsov, *Phys. Rev. Lett.*, 2004, **93**, 238103.

37. Y. Zubavichus, A. Shaporenko, V. Korolkov, M. Grunze and M. Zharnikov, *J. Phys. Chem. B*, 2008, **112**, 13711-13716.

38. H. S. Kato, M. Furukawa, M. Kawai, M. Taniguchi, T. Kawai, T. Hatsui and N. Kosugi, *Phys. Rev. Lett.*, 2004, **93**, 086403.

39. D. V. Vyalikh, V. V. Maslyuk, A. Blüher, A. Kade, K. Kummer, Y. S. Dedkov, T. Bredow, I. Mertig, M. Mertig and S. L. Molodtsov, *Phys. Rev. Lett.*, 2009, **102**, 098101.

40. S. O. Kelley, J. K. Barton, N. M. Jackson, L. D. McPherson, A. B. Potter, E. M. Spain, M. J. Allen and M. G. Hill, *Langmuir*, 1998, **14**, 6781-6784.

41. B. Gohler, V. Hamelbeck, T. Z. Markus, M. Kettner, G. F. Hanne, Z. Vager, R. Naaman and H. Zacharias, *Science*, 2011, **331**, 894-897.

42. S. G. Ray, S. S. Daube, G. Leitus, Z. Vager and R. Naaman, *Phys. Rev. Lett.*, 2006, **96**, 036101.

43. T. Z. Markus, S. S. Daube and R. Naaman, *J. Phys. Chem. B*, 2010, **114**, 13897-13903.

44. K. Fujii, K. Akamatsu, Y. Muramatsu and A. Yokoya, *Nucl. Instr. Meth. B*, 2003, **199**, 249-254.

45. T. Oka, A. Yokoya, K. Fujii, Y. Fukuda and M. Ukai, *Phys. Rev. Lett.*, 2012, **109**, 213001.

46. A. Opdahl, D. Y. Petrovykh, H. Kimura-Suda, M. J. Tarlov and L. J. Whitman, *Proc. Nat. Acad. Sci.*, 2007, **104**, 9-14.

47. S. Ptasinska, A. Stypczynska, T. Nixon, N. J. Mason, D. V. Klyachko and L. Sanche, *J. Chem. Phys.*, 2008, **129**, 065102-065106.

48. D. Y. Petrovykh, H. Kimura-Suda, L. J. Whitman and M. J. Tarlov, *J. Am. Chem. Soc.*, 2003, **125**, 5219-5226.

49. B. Ravel, Chicago, 0.8.56 edn., 2009, pp. x-ray absorption spectra curve fitting.

50. T. M. Herne and M. J. Tarlov, *J. Am. Chem. Soc.*, 1997, **119**, 8916-8920.

51. M. Erdmann, R. David, A. R. Fornof and H. E. Gaub, *Nat. Chem.*, 2010, **2**, 745-749.

52. D. V. Leff, L. Brandt and J. R. Heath, *Langmuir*, 1996, **12**, 4723-4730.

53. L. Venkataraman, J. E. Klare, C. Nuckolls, M. S. Hybertsen and M. L. Steigerwald, *Nature*, 2006, **442**, 904-907.

54. F. Chen, X. Li, J. Hihath, Z. Huang and N. Tao, *J. Am. Chem. Soc.*, 2006, **128**, 15874-15881.

55. G. Ceballos, H. Wende, K. Baberschke and D. Arvanitis, *Surf. Sci.*, 2001, **482-485**, 15-20.

56. D. V. Klyachko, M. A. Huels and L. Sanche, *Radiat. Res.*, 1999, **151**, 177-187.

57. F. Xiao, X. Luo, X. Fu and Y. Zheng, *J. Phys. Chem. B*, 2013, **117**, 4893-4900.

58. N. Mirsaleh-Kohan, A. D. Bass and L. Sanche, *J. Chem. Phys.*, 2011, **134**, 015102-015108.

59. T. M. Orlando, D. Oh, Y. Chen and A. B. Aleksandrov, *J. Chem. Phys.*, 2008, **128**, 195102-195107.

60. M. R. Vilar, A. M. Botelho do Rego, A. M. Ferraria, Y. Jugnet, C. Noguès, D. Peled and R. Naaman, *J. Phys. Chem. B*, 2008, **112**, 6957-6964.

61. L. Sanche, *Eur. Phys. J. D*, 2005, **35**, 367-390.

62. J. Simons, *Acc. Chem. Res.*, 2006, **39**, 772-779.

63. K. Fujii, K. Akamatsu and A. Yokoya, *Int. J. Radiat. Biol.*, 2004, **80**, 909-914.

64. M. Wolf, S. Nettesheim, J. M. White, E. Hasselbrink and G. Ertl, *J. Chem. Phys.*, 1991, **94**, 4609-4619.

65. S. Ptasinska, S. Denifl, P. Scheier and T. D. Mark, *J. Chem. Phys.*, 2004, **120**, 8505-8511.

66. R. Panajotovic, F. Martin, P. Cloutier, D. Hunting and L. Sanche, *Radiat. Res.*, 2006, **165**, 452-459.

67. T. Z. Markus, M. Wu, L. Wang, D. H. Waldeck, D. Oron and R. Naaman, *J. Phys. Chem. C*, 2009, **113**, 14200-14206.

68. Y. Zheng, P. Cloutier, D. J. Hunting, L. Sanche and J. R. Wagner, *J. Am. Chem. Soc.*, 2005, **127**, 16592-16598.

69. Y. Zheng, P. Cloutier, D. J. Hunting, J. R. Wagner and L. Sanche, *J. Chem. Phys.*, 2006, **124**, 064710-064719.

70. Y. Zheng, J. R. Wagner and L. Sanche, *Phys. Rev. Lett.*, 2006, **96**, 208101.

71. F. Martin, P. D. Burrow, Z. Cai, P. Cloutier, D. Hunting and L. Sanche, *Phys. Rev. Lett.*, 2004, **93**, 068101.

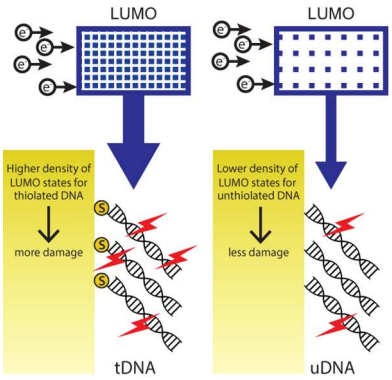

Table of Contents Image

Illustration showing that secondary electrons have a higher damage probability for thiolated DNA as opposed to unthiolated DNA, due to the former's higher density of LUMO states, which leads to more efficient capture of the low energy electrons.

Supplementary information on polarization modulation infrared reflection absorption spectroscopy (PM-IRRAS) of tDNA and uDNA

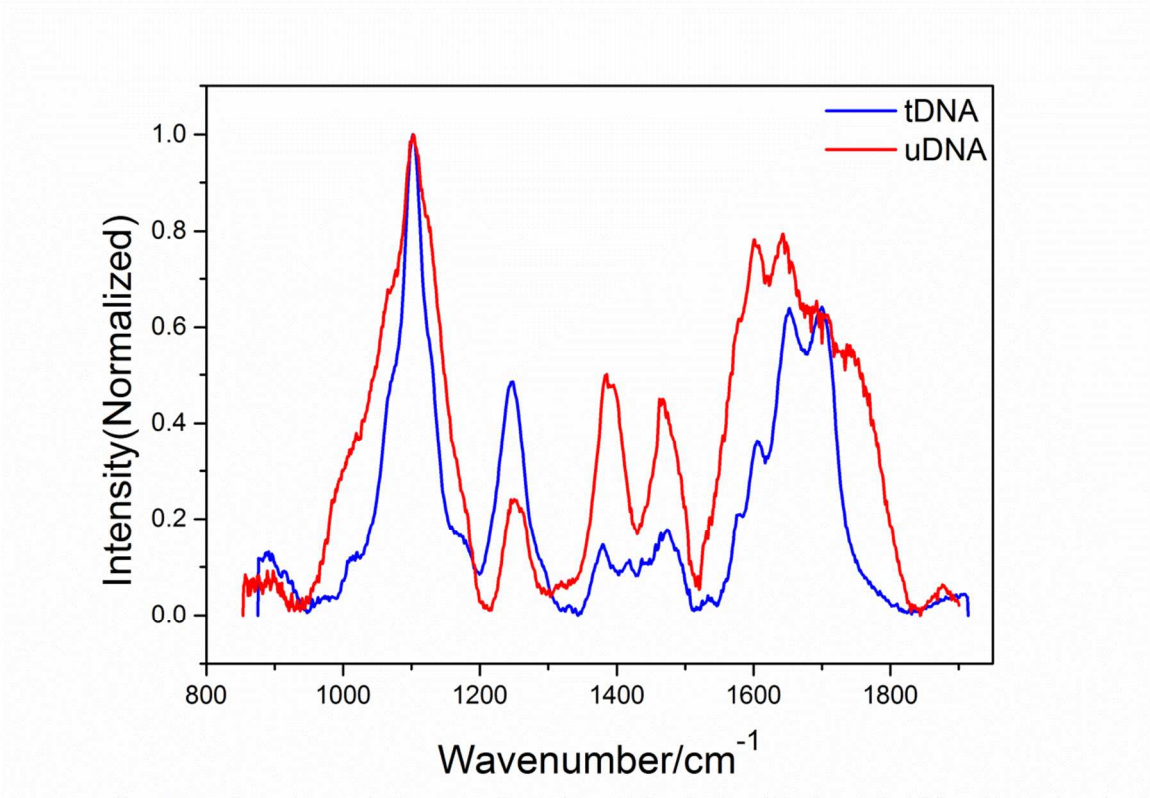

Figure 1: PM-IRRA Spectra of monolayers of t-DNA and u-DNA on Au at an incidence angle of 80^0.

Infrared absorption spectra of tDNA and uDNA were recorded in reflection mode at an incidence angle of 80^0 using a Nicolet 6700 FTIR, equipped with PEM-90 photo elastic modulator (Hinds Instruments, Hillsboro, OR). The peaks, which are centered at 1100 and 1246 cm^{-1}, represents the symmetric and asymmetric PO_2^- stretching vibration of the DNA phosphodiester backbone. The peaks at 1464 result from the purine (DNA bases) ring modes, whereas the band in the region

from 1600 to 1750 cm^{-1} is due to the C=O and C=N stretching and $-NH_2$ bending vibrations of the thymine and adenine bases in the DNA. The strong band at 1604 cm^{-1} in uDNA spectra shows that DNA bases interact with gold surface directly.[1] The change in the peak positions with the thiolated and non-thiolated DNA has previously been reported by Opdahl *et al.*,[2] who also found that in the case of thymine bases, which do not directly interact with the gold substrate, there is a band at 1700 cm−1.

1. K.S. Kumar and R. Naaman, *Langmuir*, 2012, **28**, 14514.

2. A. Opdahl, D. Y. Petrovykh, H. Kimura-Suda, M. J. Tarlov and L. J. Whitman, *Proc. Nat. Acad. Sci.*, 2007, **104**, 9-14.

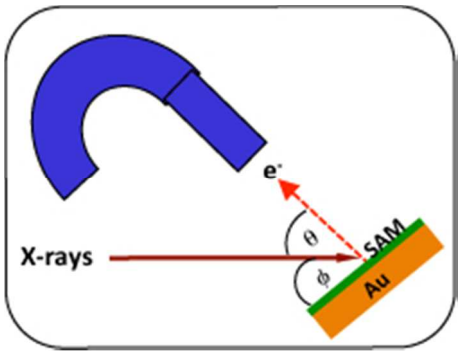

Figure 1. Schematic diagram of the experimental setup.
79x60mm (72 x 72 DPI)

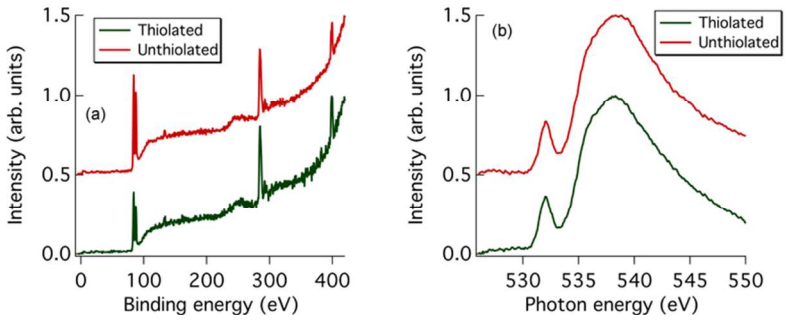

Figure 2. (a) Survey XPS spectra of thiolated (bottom) and unthiolated (top) DNA adsorbed on Au taken with 500 eV photons at the SRC. (b) O 1s X-ray absorption spectra of thiolated (bottom) and unthiolated (top) DNA adsorbed on Au taken at the APS.
83x62mm (300 x 300 DPI)

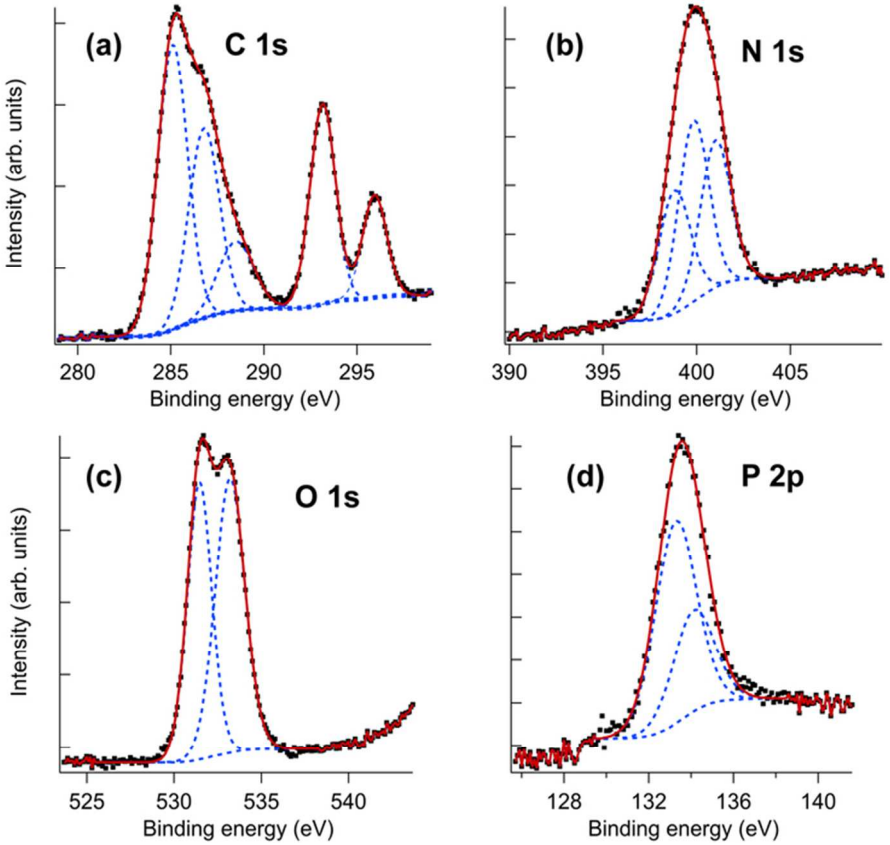

Figure 3. Core level XPS of thiolated DNA adsorbed on Au taken with 950 eV X-rays at the APS. (a) C 1s and K 2p (b) N 1s (c) O 1s (d) P 2p. The points are the experimental data, the dashed lines are fits to individual components (see Table 1) and the solid line is the fitted envelope.
70x60mm (300 x 300 DPI)

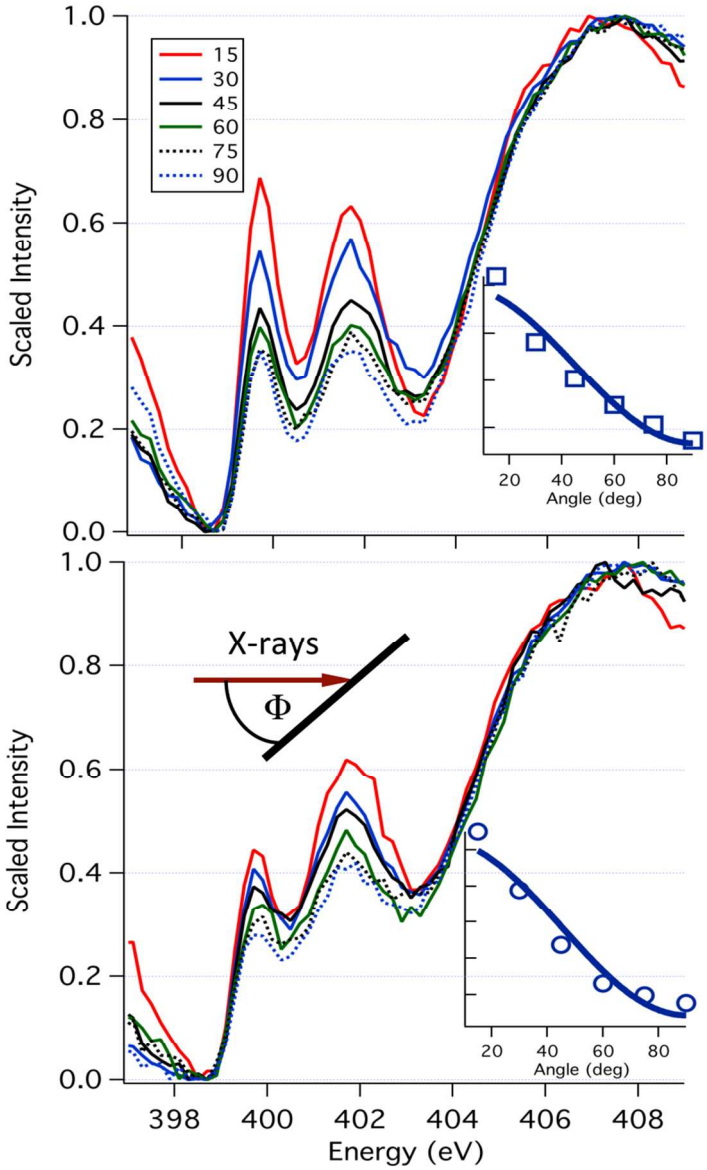

Figure 4. Polarization-dependent N 1s X-ray absorption spectra of thiolated (top) and unthiolated (bottom) DNA adsorbed on Au taken at the SRC. The insets show the angular dependence of the π* resonance at 399 eV for thiolated DNA and 401 eV for unthiolated DNA. The symbols are the experimental data and the straight line is a fit to the model discussed in the text.
81x126mm (300 x 300 DPI)

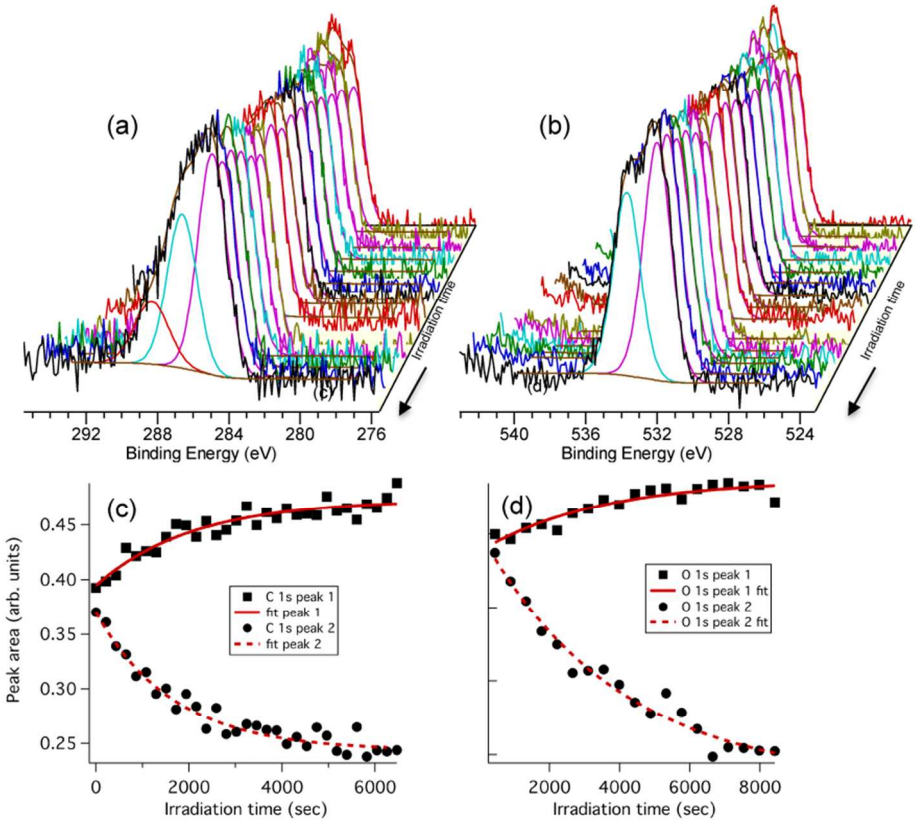

Figure 5. Series of irradiation time-dependent XP spectra: (a) C 1s (b) O 1s. Also shown are the deconvoluted spectral components. Irradiation time dependence of the areas of peaks 1 and 2 (see Table 1) for (c) C 1s (d) O 1s. The symbols are the experimental data and the straight line is a fit to the model discussed in the text.
81x67mm (300 x 300 DPI)